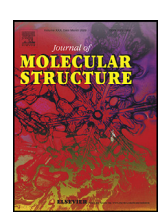
ELSEVIER

Contents lists available at ScienceDirect

#### Journal of Molecular Structure

journal homepage: www.elsevier.com/locate/molstr



## Two high-spin cobalt(III) complex anions with pyridinium-based cations: synthesis, structural elucidation and magnetic properties



Ledoux S. Pouamo<sup>a</sup>, Carole F.N. Nguemdzi<sup>b</sup>, Mohammad Azam<sup>c</sup>, Diana Luong<sup>d</sup>, Kate A. Gibson<sup>d</sup>, Wangxiang Li<sup>d</sup>, Elena B. Haddon<sup>d</sup>, Boniface P.T. Fokwa<sup>d,\*</sup>, Justin Nenwa<sup>a,\*</sup>

- <sup>a</sup> Inorganic Chemistry Department, University of Yaounde 1, PO Box 812, Yaounde, Cameroon
- <sup>b</sup> Department of Chemistry, University of Bamenda, PO Box 39, Bambili, Cameroon
- <sup>c</sup> Department of Chemistry, College of Science, King Saud University, PO Box 2455, Riyadh 11451, Saudi Arabia
- <sup>d</sup> Chemistry Department, University of California Riverside, 501 Big Springs Rd, Riverside, CA 92521, USA

#### ARTICLE INFO

# Article history: Received 6 May 2022 Revised 10 June 2022 Accepted 14 June 2022 Available online 21 June 2022

Keywords: Hybrid salts Oxalate(2-) anion High-spin cobalt(III) Pyridinium cations Magnetism

#### ABSTRACT

Two novel hybrid salts containing high spin tris(oxalato)cobaltate(III) complexes and pyridinium derivative isomer cations, viz.  $(C_7H_{11}N_2)_3[Co(C_2O_4)_3]\cdot nH_2O$   $(C_7H_{11}N_2^+=2-amino-4,6-dimethylpyridinium)$ cation, n = 0 for salt 1;  $C_7H_{11}N_2^+ = 4$ -dimethylaminopyridinium, n = 4 for salt 2) were successfully isolated from aqueous solution. They were characterized using various physicochemical techniques, such as C, H, N microanalyses, thermogravimetric studies, FT-IR, UV-Vis, EDX, PXRD, single-crystal X-ray crystallography, and SQUID magnetometry. The size of the pyridinium derivative isomer cations has a major impact on the crystal structures. Salt 1 has a 3-D supramolecular framework formed by O-H···O hydrogen bonds between the high-spin [Co(C2O4)3]3- complex anion and the sterically encumbering 2-amino-4,6dimethylpyridinium cations. The 3-D supramolecular framework of salt 2 is comprised of  $[Co(C_2O_4)_3]^{3-1}$ complex anion, small size 4-dimethylaminopyridinium cations and uncoordinated water molecules via N-H···O and O-H···O hydrogen bonds. Structural cohesion is reinforced by  $\pi$ - $\pi$  stacking interactions between the pyridine rings in both salts. Temperature-dependence magnetic moment  $(\mu)$  collected under zero-field cooled (ZFC) and field-cooled (FC) conditions revealed robust antiferromagnetic ordering below  $T_{\rm N}=25$  K. The negative Weiss constant,  $\theta=-55$  K, confirmed the presence of antiferromagnetic interactions between Co(III) ions at low temperatures in 1 and the estimated effective magnetic moment of 4.5  $\mu_{\rm B}$  supports the presence of the rare Oh high-spin Co(III) in this hybrid salt.

© 2022 Elsevier B.V. All rights reserved.

#### 1. Introduction

Organic-inorganic hybrid salts (OIHS) are fascinating crystalline materials comprised of organic cations and their inorganic counterparts. In contrast to classical salts formed by rigid entities put together solely by electrostatic interactions, modern supramolecular systems with novel solid-state architectures are largely made up of non-covalent intermolecular interactions [1,2]. These secondary interactions include hydrogen bonding,  $\pi$ - $\pi$  and van der Waals forces and occupy a prominent position in the cohesion of the structures [3–8]. During the last decades, OIHSs have emerged as a new class of exciting functional materials that combine the versatility of both the organic and the inorganic components and have been widely applied to various fields, such as non-linear optics

E-mail addresses: bfokwa@ucr.edu (B.P.T. Fokwa), jnenwa@yahoo.fr (J. Nenwa).

[9,10], metallic conductivity [11,12], catalysis [13] and magnetism [14–16].

Paramagnetic compounds have been investigated for a long time mainly because of their exceptional magnetic properties [17,18]. Depending on the strength of the ligand, octahedral Co(III) complexes may exist as diamagnetic (low-spin),  $t_{2g}^{\ 6}e_{g}^{\ 0}$  and/or paramagnetic (high-spin),  $t_{2g}^{\ 4}e_{g}^{\ 2}$  configuration. Until now, despite its appealing magnetic properties, very little is known concerning paramagnetic octahedral Co(III) complexes, in contrast to a huge number of diamagnetic Co(III) complexes with various organic ligands [19–23].

The present work stems from our interest to design and study the magnetic properties of high-spin metal(III) complexes of carboxylate(2-) ligands like oxalate(2-) anion,  $C_2O_4^{2-}$ . Recently, we have been concerned with the synthesis and properties of some OIHSs with general formula  $(Org-H)_3[M^{III}(C_2O_4)_3]\cdot nH_2O$   $(Org-H^+=$  protonated organic molecule, M= Cr(III), Fe(III)) [24–26]. Such salts may be used as appropriate precursors for the development of multifunctional systems in which small in-

<sup>\*</sup> Corresponding authors:

**Table 1**Crystal data and structure refinement results for **1** and **2**.

Compound	1	2
Empirical formula	$C_{27}H_{33}CoN_6O_{12}$	C <sub>27</sub> H <sub>41</sub> CoN <sub>6</sub> O <sub>16</sub>
Formula weight	692.52	764.59
T (K)	293(2)	293(2)
λ (Å)	0.71073	0.71073
Crystal system	Triclinic	Monoclinic
Space group	P-1 (no. 2)	C2/c (no. 15)
Unit Cell parameters	, ,	
a (Å)	11.227(2)	18.827(2) Å
b (Å)	11.368(2)	16.6476(16)
c (Å)	12.722(2)	11.0305(11)
α (°)	84.13(2)	90
β (°)	84.13(2)	98.63(1)
γ (°)	82.74(2)	90
$V(\mathring{A}^3)$	1602.2(4)	3418.1(6)
Z	2	4
$\mu \text{ (mm}^{-1}\text{)}$	1.435	1.486
F(0 0 0)	720	1532
Crystal size (mm)	$0.336 \times 0.247 \times 0.128$	$1.895 \times 0.52 \times 0.45$
$\theta$ range for data collection	2.796 - 28.340	3.079 - 33.549
(°)		
Index ranges	-14 < h < 14, -13 < k < 15,	-27 < h < 28, -17 < k < 25,
8	-16 < l < 16	-9 < l < 16
Total reflections $(R_{int})$	10681 (0.0736)	9659 (0.044)
Unique reflections	7883	5896
Refinement method	full-matrix least squares on $F^2$	full-matrix least squares on $F^2$
Data/restraints/parameters	7883/ 8/ 447	5896/0/ 250
Goodness-of-fit (GOF) on	0.958	1.056
$F^2$		
R factor $[I > 2\sigma(I)]$	$R_1 = 0.0841, wR_2 = 0.1818$	$R_1 = 0.0792$ , $wR_2 = 0.1430$
R factor (all data)	$R_1 = 0.1860, \text{ w}R_2 = 0.2406$	$R_1 = 0.1840, \text{ w}R_2 = 0.1904$
Max and min residual	0.479 and -0.402	0.680 and -556
electron density (e/ų)		

organic species like hydronium  $(H_3O^+)$  ions may replace sterically encumbering organic cations. Materials of this type, no doubt, could be well-adapted model in the exploration of the concept of one-dimensional proton conducting solid (1D-PCS) [27–30]. In continuation of the research work on tris(oxalato)metalate(III) hybrid salts, we herein report two novel systems containing the high-spin tris(oxalato)cobaltate(III) complexes and the pyridinium derivative isomer cations, viz.  $(C_7H_{11}N_2)_3[Co(C_2O_4)_3]\cdot nH_2O(C_7H_{11}N_2^+=2\text{-amino-4,6-dimethylpyridinium cation, }n=0$  for salt 1;  $C_7H_{11}N_2^+=4\text{-dimethylaminopyridinium, }n=4$  for salt 2). These rare paramagnetic Co(III) salts have been spectroscopically characterized and structurally confirmed by single crystal X-ray diffraction. Their thermal behavior and magnetic properties have also been investigated.

#### 2. Experimental

#### 2.1. Materials and physical measurements

All reagents were used as received unless otherwise stated. The paramagnetic precursor salt  $K_3[Co(C_2O_4)_3]\cdot 3H_2O$ , green color, was prepared as described in the literature [31]. A Perkin-Elmer 240C analyzer and Philips XL 30 FEG scanning electron microscope fitted with an EDAX SiLi detector were used for C, H, N and energy-dispersive X-ray spectroscopy (EDX), respectively. Alpha-P Bruker FT-IR spectra was used to record the FT-IR spectra as a KBr pellet at 4000–400 cm<sup>-1</sup>, whereas UV/Vis HACH/Series DR 3900 spectrophotometer was utilized to conduct UV/Vis studies. An LIN-SEIS STA PT-1000 thermal analyzer was used to conduct simultaneous TG/DSC measurements in air at temperature 10°C per minute. A Bruker D8 Advance powder diffractometer equipped with a 40 kV, 40 mA Cu  $K\alpha$  radiation ( $\lambda$  = 1.5418 Å) was used to record powder X-ray diffraction patterns. The sample was finely pulverized and put into an aluminum tray with the parameters: angular

range: 5–80°; step: 0.02; integration time: 0.5 s. In cases where single-crystal structures were available, these spectra were compared to those derived from them. In a cryogen-free version of the EverCool-II physical property measurement system (QDI, USA) samples were measured using vibrating magnetometers. To avoid anisotropic orientation, approximately 30 mg tightly packed and sealed powered polycrystalline samples of 1 and 2 were magnetized *versus* temperature at 100 Oe down to 4 K. Pascal's constants were used for the diamagnetic corrections of all constituent atoms and the contributions from the sample holders [32].

#### 2.2. Syntheses of salts 1 and 2

#### 2.2.1. Synthesis of $(C_7H_{11}N_2)_3[Co(C_2O_4)_3]$ (1)

 $K_3[Co(C_2O_4)_3]\cdot 3H_2O$  (990 mg, 2 mmol), oxalic acid  $H_2C_2O_4\cdot 2H_2O$  (400 mg, 3.2 mmol) and 2-amino-4,6-dimethylpyridine (730 mg, 6 mmol) were added in deionized water (50 mL). Afterward, the resulting mixture was agitated for one hour at  $40^{\circ}C$  under ambient conditions before cooling at r.t. and filtering. The green filtrate was kept at r.t. under the hood. Dark-green prismatic crystals appropriate for X-ray diffraction were obtained after three weeks. Yield: 872 mg (1.26 mmol, 63%). Anal. Calcd. For  $C_{27}H_{33}CoN_6O_{12}$  (1) (%): C, 46.83; H, 4.80; N, 12.14. Found (%): C, 46.87; H, 4.69; N, 12.05. IR data (cm<sup>-1</sup>): 3323 (w), 3160 (w), 1635 (s), 1607 (s), 1390 (s), 442 (s) (Fig. S1). UV-Vis (H<sub>2</sub>O, nm): 425; 604 (Fig. S3).

#### 2.2.2. Synthesis of $(C_7H_{11}N_2)_3[C_0(C_2O_4)_3]\cdot 4H_2O$ (2)

Following the above procedure as mentioned for salt **1**, salt **2** was prepared by substituting 4-dimethylaminopyridine (730 mg, 6 mmol) for 2-amino-4,6-dimethylpyridine. After three weeks, dark-green prism shaped crystals appropriate for X-ray diffraction were extracted. Yield: 994 mg (1.30 mmol, 65%). Anal. Calcd. for  $C_{27}H_{41}CoN_6O_{16}$  (%): C, 42.41; H, 5.40; N, 10.99. Found (%): C, 42.39; H, 5.34; N, 11.04. IR data (cm<sup>-1</sup>): 3550 (w), 3378 (w), 3067 (w),

1<sup>st</sup> step: Protonation of imine groups of the pyridine derivatives (Py)

$$2 \text{ Py} + \text{H}_2\text{C}_2\text{O}_4 \xrightarrow{\text{H}_2\text{O}} (\text{Py-H})_2\text{C}_2\text{O}_4$$

2<sup>nd</sup> step: Exchange of K<sup>+</sup> with (Py-H)<sup>+</sup>

$$3(Py-H)_2C_2O_4 + 2K_3[Co(C_2O_4)_3] \cdot 3H_2O \xrightarrow{H_2O}$$
  
 $2(Py-H)_3[Co(C_2O_4)_3] \cdot nH_2O + 3K_2C_2O_4$ 

Scheme 1. Two-step formation of salts 1 and 2

1644 (s), 1603 (s), 1377 (s), 440 (s) (Fig. S2). UV-Vis (H<sub>2</sub>O solution, nm): 425; 604 (Fig. S4).

#### 2.3. X-ray crystallographic data collection and refinement

Bruker APEX II CCD diffractometer equipped with Mo-K $\alpha$  radiation ( $\lambda=0.71073$  Å) was operated to find the single-crystal intensity data for 1 and 2. A semi-empirical procedure was used to correct the X-ray intensities for absorption [33]. The SHELX-2014 package was used to solve both structures directly and refine them using full-matrix least-square techniques on  $F^2$  [34]. Anisotropic refinement was used for all non-hydrogen atoms. The remaining position of C–H atoms was determined using geometrical and riding models. The crystallographic data were processed with the Diamond [35] and PublCIF [36] programs. All of the crystallographic and refining details are listed in Table 1.

#### 3. Results and discussion

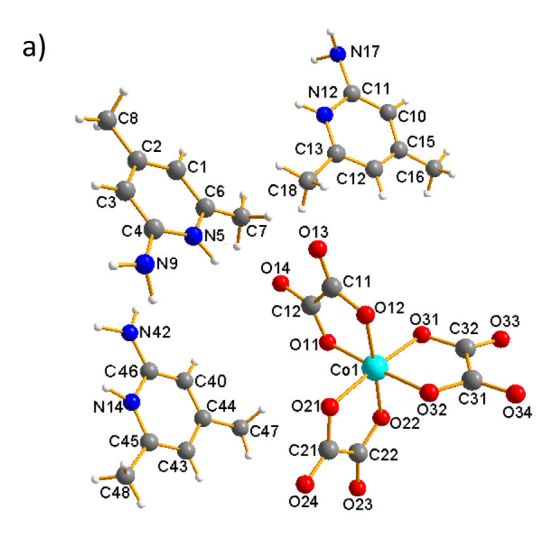
#### 3.1. Synthesis of 1 and 2

The  $(C_7H_{11}N_2)_3[Co(C_2O_4)_3]$ target salts **(1)**  $(C_7H_{11}N_2)_3[Co(C_2O_4)_3]\cdot 4H_2O$  (2), both green color, were formed in a two-step process (Scheme 1). In the first step, the oxalic acid protonates the imine groups of pyridine derivatives (Py), yielding iminium cations (Pv-H)+, while in the second step, the potassium cations of the precursor salt K<sub>3</sub>[Co(C<sub>2</sub>O<sub>4</sub>)<sub>3</sub>].3H<sub>2</sub>O are exchanged with iminium cations. The EDX spectra (Fig. S5) and elemental analyses of both salts support the single-crystal X-ray findings. Salts 1 and 2 are air-sensitive, easily soluble in water and sparingly soluble in a mixture of water/ethanol. It is worth noting that salts from this family are also sensitive to the protonating acid used and to the reaction stoichiometry [37,38].

#### 3.2. Structure description of 1 and 2

A single-crystal structure analysis reveals that the hybrid salts  $(C_7H_{11}N_2)_3[Co(C_2O_4)_3]$  (1) and  $(C_7H_{11}N_2)_3[Co(C_2O_4)_3]$ ·4H<sub>2</sub>O (2) crystallize in the triclinic *P*-1 space group and monoclinic *C2/c* space group, respectively. The crystal structure details of 1 and 2 are depicted in Fig. 1, with each cobalt atom in a six-coordinate environment.

The crystal structure of  $\mathbf{1}$  (Fig. 1a) consists of one tris(oxalato)cobaltate(III) anion  $[Co(C_2O_4)_3]^{3-}$  and three 2-amino-4,6-dimethylpyridinium cations  $(C_7H_{11}N_2)^+$  compensating the charge of the complex anion. Selected bond lengths and angles around the cobalt(III) ions are listed in Table 2. The central Co(III) ion forms a coordination sphere consisting of six O atoms from three chelating oxalate(2-) ligands in a distorted (2+2+2) octahedral arrangement. The salt  $(C_7H_{11}N_2)_3[Co(C_2O_4)_3]$  (1) is isostructural to its homologues  $(C_7H_{11}N_2)_3[Cr(C_2O_4)_3]$  [25] and  $(C_7H_{11}N_2)_3[Fe(C_2O_4)_3]$  [26]. The Co-O distances range from



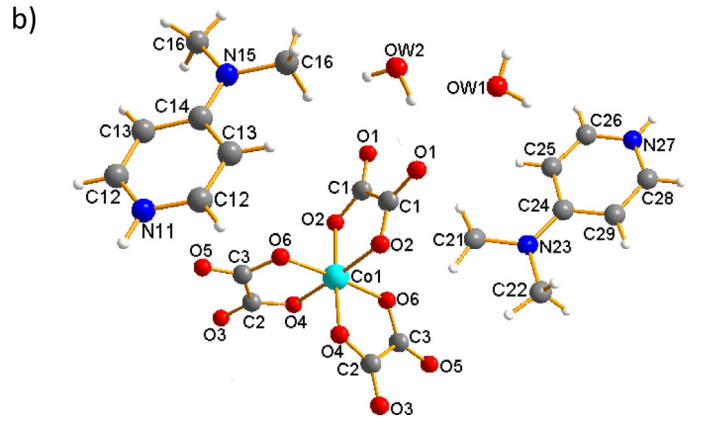


Fig. 1. Constitutive entities of 1 (a) and 2 (b) with the atom numbering scheme.

Table 2 Selected bond distances (Å) and angles (°) for compounds 1 and 2.

selected bond distances (11) and angles ( ) for compounds I and 2.							
$(C_7H_{11}N_2)_3[Co(C_2$	$C_7H_{11}N_2)_3[C_0(C_2O_4)_3]$ (1)						
Co1-O11	1.878(4)	021-Co1-022	85.95(17)				
Co1-O12	1.876(4)	012-Co1-032	91.09(18)				
Co1-O21	1.892(4)	011-Co1-032	176.81(18)				
Co1-O22	1.895(4)	021-Co1-032	90.53(17)				
Co1-O31	1.915(4)	022-Co1-032	90.48(17)				
Co1-O32	1.906(4)	012-Co1-031	91.57(17)				
012-Co1-011	86.56(18)	011-Co1-031	91.55(18)				
012-Co1-021	92.42(17)	021-Co1-031	174.98(17)				
011-Co1-021	91.73(18)	022-Co1-031	90.14(16)				
012-Co1-022	177.75(17)	032-Co1-031	86.35(18)				
011-Co1-022	91.93(17)						
$(C_7H_{11}N_2)_3[Co(C_2)$	$_{7}H_{11}N_{2})_{3}[Co(C_{2}O_{4})_{3}]\cdot 4H_{2}O$ (2)						
Co1-O4	1.883(2)	06 <sup>i</sup> -Co1-O6	176.3 (2)				
Co1-O4 <sup>i</sup>	1.883(2)	04-Co1-O2i	177.2(2)				
Co1-O6 <sup>i</sup>	1.889(2)	04 <sup>i</sup> -Co1-O2 <sup>i</sup>	91.8(1)				
Co1-O6	1.889(2)	06 <sup>i</sup> -Co1-O2 <sup>i</sup>	91.3(2)				
Co1-O2i	1.899(2)	06-Co1-O2 <sup>i</sup>	91.4(2)				
Co1-O2	1.899(2)	04-Co1-O2	91.8(1)				
04-Co1-O4 <sup>i</sup>	90.1(2)	04 <sup>i</sup> -Co1-O2	177.2(2)				
04-Co1-06 <sup>i</sup>	86.73(1)	06 <sup>i</sup> -Co1-O2	91.4(2)				
04 <sup>i</sup> -Co1-O6 <sup>i</sup>	90.6(1)	06-Co1-O2	91.2(2)				
04-Co1-06	90.6(1)	02 <sup>i</sup> -Co1-O2	86.3(2)				
04 <sup>i</sup> -Co1-O6	86.7(1)						

Symmetry transformations used to generate equivalent atoms: (i) -x, y, 0.5-z; (ii) 1-x, y, 0.5-z.

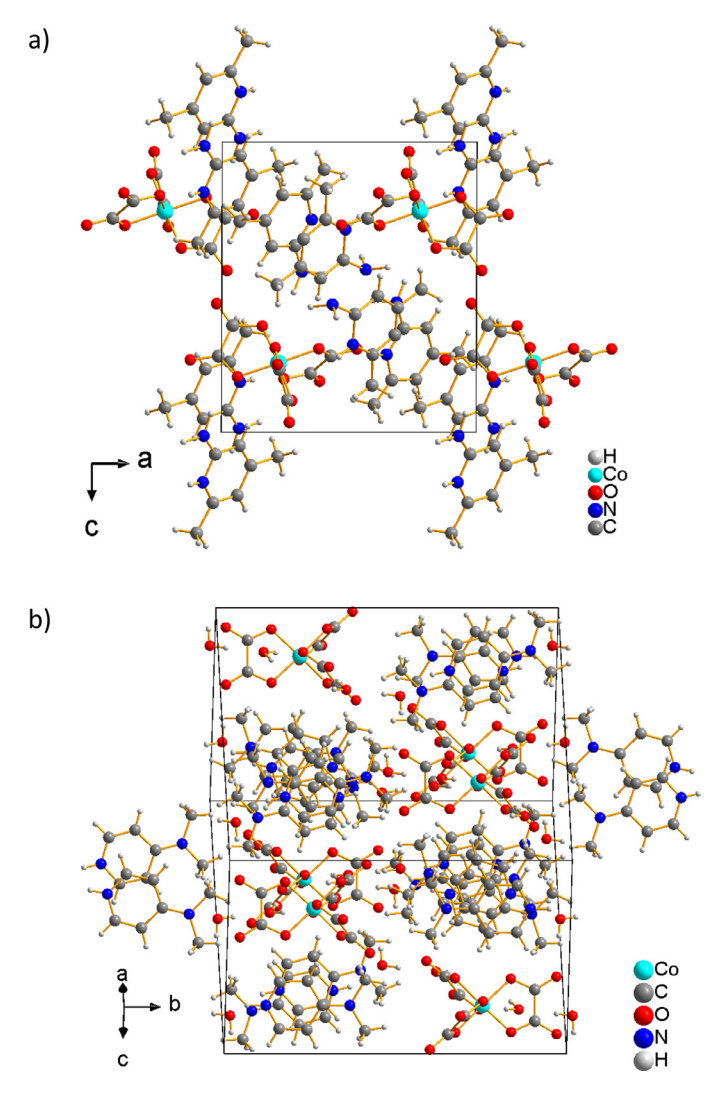
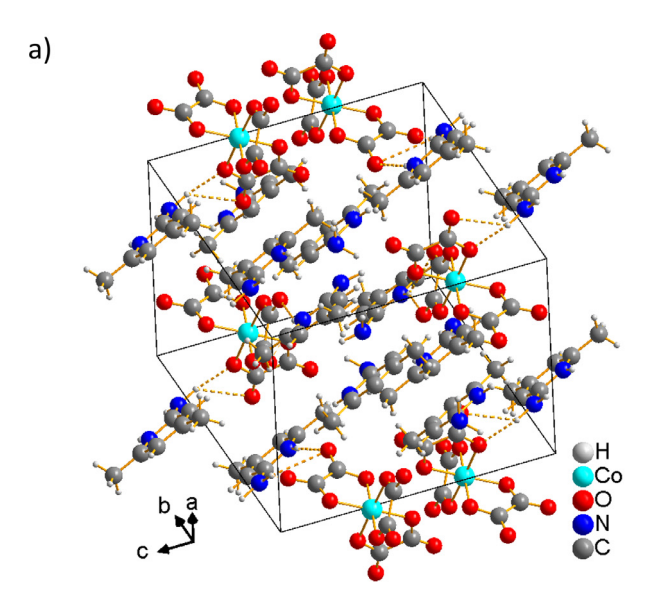
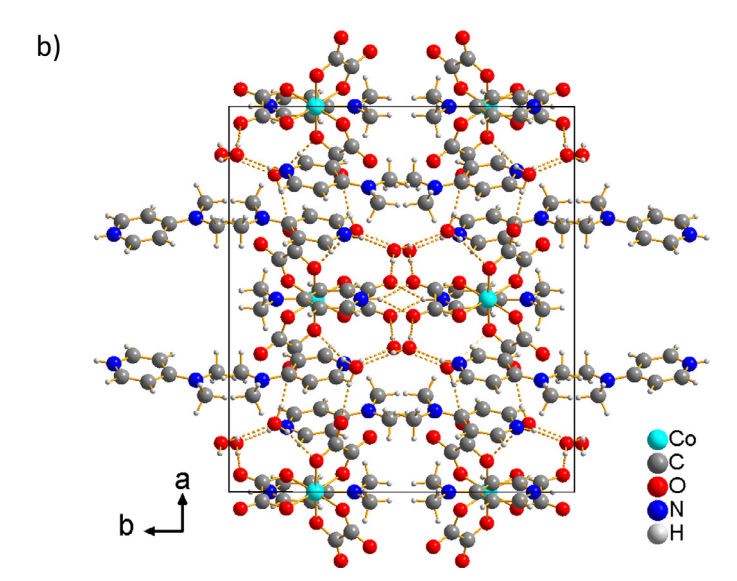


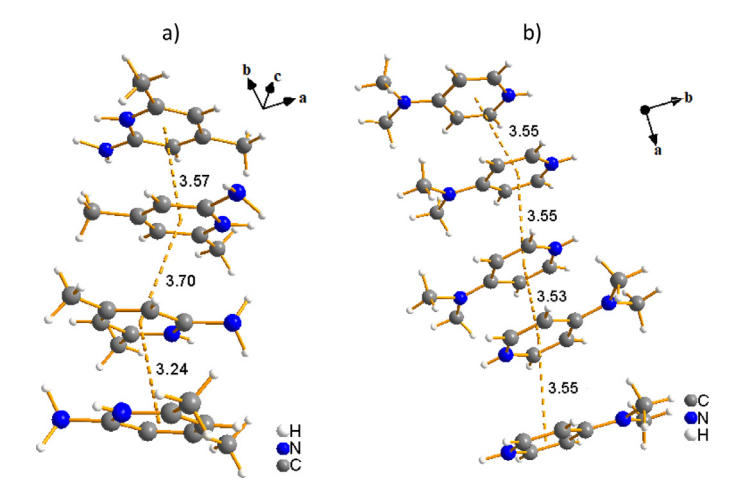
Fig. 2. Packing diagrams of  ${\bf 1}$  (a) and  ${\bf 2}$  (b) illustrating columns of cations and anions.

1.876(4) [Co1-O12] to 1.915(4) Å [Co1-O31], and the O-Co-O angles from 85.95(17) [O21-Co1-O22] to 177.75(17)° [O12-Co1-O22]. These geometric parameters are comparable to those found in homologous compounds containing  $[M(C_2O_4)_3]^{3-}$  anionic units [25,26]. The  $(C_7H_{11}N_2)^+$  cation has the same geometric parameters as similar salts that involve the same cationic entity [25,26]. The packing diagram of 1 is shown in Fig. 2a, with columns of cations and anions. Extended H-bonds connecting ionic entities in 1 are highlighted in Fig. 3a. In the crystal, the protonated nitrogen atoms N05 and N042 are involved in moderate intermolecular hydrogen bonding interactions with the oxygen atoms O13 and O22<sup>ii</sup>, respectively, with N-O distances ranging from 2.814(7) [N05-H05-013] to 2.973(7) Å [N042-H42A-022ii]. Hydrogen bond parameters for 1 and 2 are summarized in Table 3. In salt **1**,  $\pi$ - $\pi$  interactions between pyridine rings (centroid-to-centroid distances of 3.24 Å and 3.70 Å) contribute to the cohesion of the three-dimensional framework (Fig. 4a). The crystal structure of 2 is depicted in Fig. 1b. It is composed of a  $[Co(C_2O_4)_3]^{3-}$  complex anion, three 4-dimethylaminopyridinium cations (C<sub>7</sub>H<sub>11</sub>N<sub>2</sub>)<sup>+</sup> and four crystallization water molecules. As in salt 1, the central Co(III) ion in 2 forms a coordination sphere made of six O atoms from three chelating oxalate(2-) ligands in a distorted (2+2+2)octahedral arrangement. The salt  $(C_7H_{11}N_2)_3[Co(C_2O_4)_3]\cdot 4H_2O$  (2) is isostructural to its homologues  $(C_7H_{11}N_2)_3[Cr(C_2O_4)_3]\cdot 4H_2O$ 

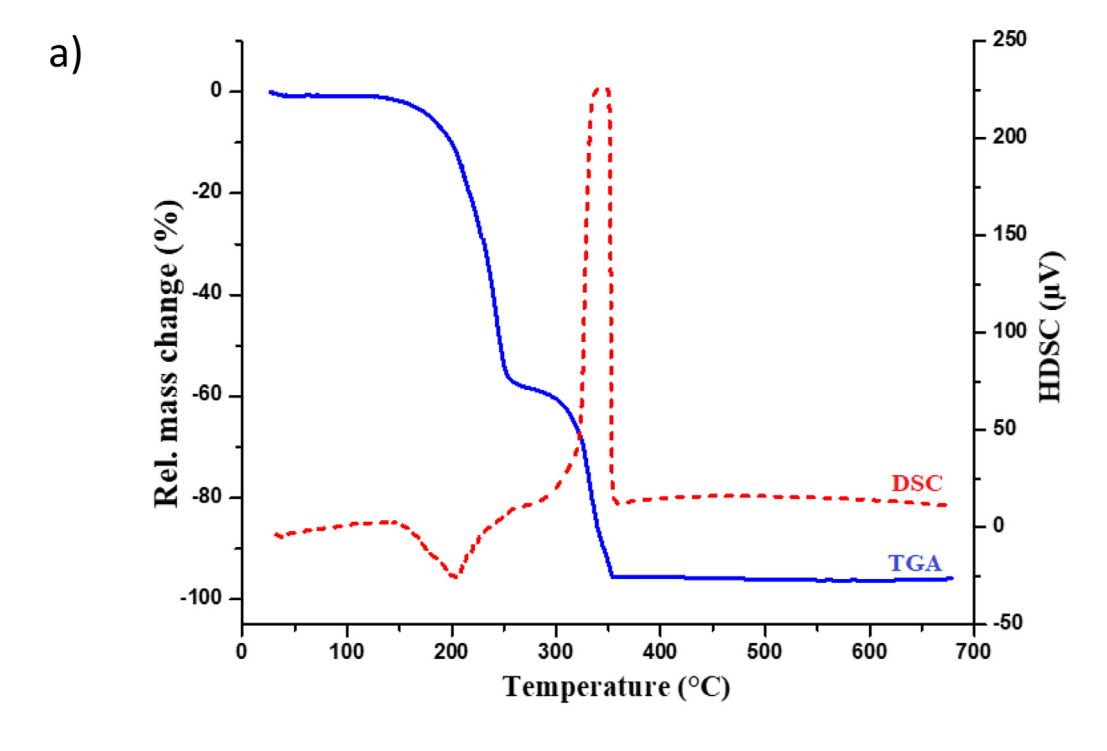




**Fig. 3.** H-bonds (dashed lines) connecting ionic entities in  $\mathbf{1}$  (a) and ionic entities and water molecules in  $\mathbf{2}$  (b).



**Fig. 4.**  $\pi$ - $\pi$  stacking interactions in **1** (*a*) and **2** (*b*).



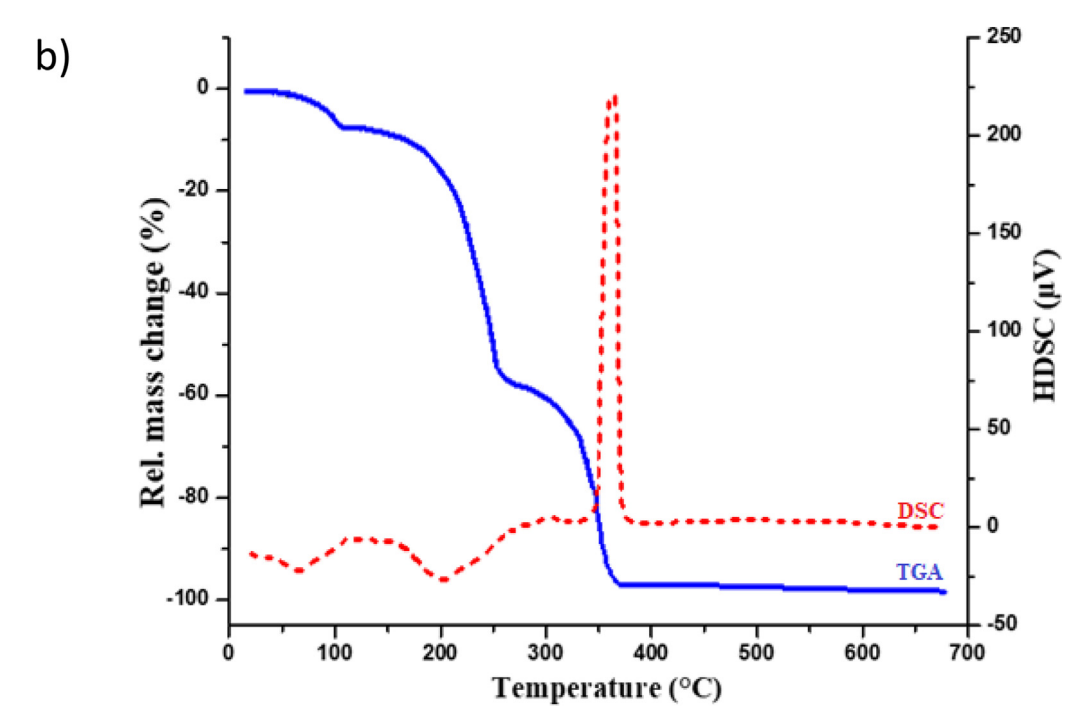


Fig. 5. TGA (blue) and DSC (red) diagrams of 1 (a) and 2 (b).

[24] and  $(C_7H_{11}N_2)_3$ [Fe( $C_2O_4)_3$ ]·4H<sub>2</sub>O [26]. The Co–O distances range from 1.883(2) [Co1–O4; Co1–O4<sup>i</sup>] to 1.899(2) Å [Co1–O2; Co1–O2<sup>i</sup>] and the O–Co–O angles from 86.3(2) [O2<sup>i</sup>–Co1–O2] to 177.2(2)° [O4–Co1–O2<sup>i</sup>]. These geometric parameters are consistent with those found in compounds containing the  $[Co(C_2O_4)_3]^{3-}$  anionic building block [39,40].

The bond distances and angles in the 4-dimethylaminopyridinium cation are similar to the values reported for salts containing the same cationic entity [24,26,41–46]. The substituted pyridinium cations in 1 and 2 are isomers with distinct sizes and shapes. The occurrence of uncoordinated water

molecules in **2** is most likely due to the relatively small size of 4-dimethylaminopyridinium cation compared to the bulky 2-amino-4,6-dimethylpyridinium cation [24,26]. Figure 2b shows the packing diagram with columns of cations and anions. Hydrogen bonds of the type N–H···O [2.704(4) to 2.882(5) Å] and O–H···O [2.746(5) to 2.919(5) Å] (Fig. 3b) stabilize the 3-D supramolecular framework by encircling  $[\text{Co}(\text{C}_2\text{O}_4)_3]^{3-}$  complex anions, 4-dimethylaminopyridinium  $\text{C}_7\text{H}_{11}\text{N}_2^+$  cations, and lattice water molecules (Table 3). In **2**,  $\pi-\pi$  interactions (centroid-to-centroid distances of 3.53 Å and 3.55 Å) reinforce the cohesion of the three-dimensional framework (Fig. 4b).

**Table 3** Hydrogen bond lengths (Å) and bond angles ( $^{\circ}$ ) for 1 and 2.

D-H···A	d(D-H)	d(H···A)	d(D···A)	< (DHA)
$(C_7H_{11}N_2)_3[Co(C_2O_4)_3]$ (1)				
N05-H05-O13	0.89(6)	2.00(6)	2.814(7)	151(5)
N05-H05-O14	0.89(6)	2.55(6)	3.237(7)	135(5)
N042-H42B-O33i	1.09(2)	1.98(2)	3.013(8)	158(3)
N042-H42A-O22 <sup>ii</sup>	1.04(1)	2.03(1)	2.973(7)	150(3)
N042-H42A-O23 <sup>ii</sup>	1.04(1)	2.63(1)	3.413(8)	132(3)
$(C_7H_{11}N_2)_3[C_0(C_2O_4)_3]\cdot 4H_2O(2)$				
N27-H27-OW1	0.85(4)	1.89(4)	2.704(4)	158(4)
N11-H11-O1 <sup>i</sup>	0.92(6)	2.12(5)	2.882(5)	139(1)
N11-H11-O1 <sup>ii</sup>	0.92(6)	2.12(5)	2.882(5)	139(1)
OW1-HW11-OW2iii	0.80(4)	1.95(4)	2.746(5)	175(4)
OW2-HW21-O5iv	0.89(5)	1.94(5)	2.818(6)	170(5)
OW2-HW22-O6	0.76(5)	2.17(5)	2.919(5)	167(6)
OW1-HW12-O1 <sup>v</sup>	0.81(5)	1.99(6)	2.802(5)	175(5)

Symmetry transformations used to generate equivalent atoms (D, donor; A, acceptor):

(i) -x, 2-y, 1-z; (ii) x, y, -1+z for 1; (i) 0.5+x, 0.5+y, z; (ii) 0.5-x, 0.5+y, 0.5-z; (iii) 0.5-x, 0.5-y, 1-z; (iv) -0.5-x, 0.5-y, -z; (v) 0.5+x, 0.5+y, 1+z for  $\bf 2$ .

### 3.3. Powder X-ray diffraction (PXRD) and thermal analyses of ${\bf 1}$ and ${\bf 2}$

Powder X-ray diffraction (PXRD) tests were carried out to determine the phase purity of the target products (Fig. S6). The experimental PXRD patterns are practically in good agreement with the simulated patterns, suggesting that the crystal structures accurately match the bulk crystal products. Thermogravimetric analysis (TGA) and differential scanning calorimetry (DSC) were used to investigate the thermal behavior of powder samples 1 and 2 in an aerobic environment at a heating rate of 10°C·min<sup>-1</sup> at the temperature range 25°C – 700°C (Fig. 5). The thermogram of 1 (Fig. 5a) demonstrates that there is no discernible change in weight as the temperature increases to approximately 150°C, which proves that solvate water is not present in 1. When heated at 150-350°C, 1 exhibits a two-step loss of weight without any significant platform as the framework decomposes, producing a black residue of Co<sub>3</sub>O<sub>4</sub> as the prominent component [47,48]. TGA curve for 2 (Fig. 5b) illustrates three regions of weight loss without any significant platforms between them. The first 9.5% weight loss begins as a result of an endothermic effect at the temperature range 75-110°C, which corresponds to the four lattice water molecules (calcd. 9.4%). As a result of framework decomposition, the second and third weight losses, corresponding to endothermic and exothermic peaks, occur at  $100-350^{\circ}$ C and yield  $Co_3O_4$  as the final black residue [47,48].

#### 3.4. Magnetic properties

The temperature dependent magnetic moment  $(\mu)$  data of 1, collected at 1000 Oe under zero-field-cooled (ZFC) and field-cooled (FC) conditions are shown in Fig. 6. The  $\chi^{-1}$  (inverse magnetic susceptibility) vs. T curves are shown in the inset. It is clear from Fig. 6 that  $\mu$  increases with decreasing temperature reaching a maximum at 25 K (Néel temperature) before decreasing, suggesting antiferromagnetic ordering that could be due to antiferromagnetic intermolecular coupling [49]. The FC  $\chi^{-1}=f(T)$  plot could be fitted by the Curie–Weiss equation,  $\chi^{-1}=T/C-\theta/C$ , leading to Curie and Weiss constants of  $C = 3.04 \text{ emu} \cdot \text{Oe}^{-1} \cdot \text{K}$  per formula unit and  $\theta = -55$  K, respectively. The highly negative value of  $\theta$ confirms the existence of dominant antiferromagnetic interactions between the cobalt(III) centers in 1 [21]. The effective magnetic moment per cobalt(III) is estimated at 300 K as  $\sim$  4.5  $\mu_{\rm B}$ , which is slightly lower than the spin-only value of  $\sim$  4.9  $\mu_{B}$  calculated for the high spin cobalt(III) ion in Oh symmetry, thus confirming the presence of the rare high spin cobalt(III) ion in Oh symmetry in 1.

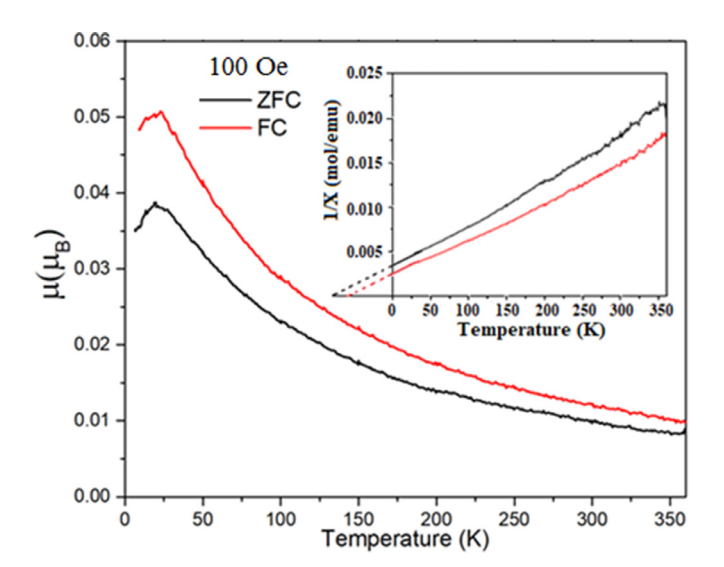


**Fig. 6.** Temperature dependence of the magnetic moment ( $\mu$ ) of **1** collected at 100 Oe under zero-field-cooled (ZFC) and field-cooled (FC) conditions. Inset shows the variation of inverse magnetic susceptibility for **1**.

#### 4. Conclusion

In summary, two novel high-spin Co(III) hybrid salts have been synthesized and fully characterized. Thermal studies confirmed the absence of crystal water in 1, due to the sterically encumbering 2amino-4,6-dimethylpyridinium cations, and their presence in compound 2, in line with the small size 4-dimethylaminopyridinium cations. Temperature-dependent magnetic moment  $(\mu)$ , collected under zero-field cooled (ZFC) and field-cooled (FC) conditions, revealed robust antiferromagnetic ordering below 25 K. The obtained negative Weiss constant confirmed the presence of antiferromagnetic interactions between Co(III) ions at low temperatures in 1. Given that the vast majority of octahedral Co(III) complexes are diamamagnetic (low spin), the present finding contributes to enlarge the rare family of high-spin Co(III) hybrid salts. The design and preparation of many other homologous materials with respect to their solid-state magnetic characteristics are of great value and now stand as a priority on the agenda of our forthcoming research

#### Credit Author statement

**Ledoux S. Pouamo:** Experiments, writing original draft. **Carole F.N. Nguemdzi:** Experiments, investigation. **Mohammad Azam:** Draft revision and editing. **Diana Luong:** Instrumental characterization. **Kate A. Gibson:** Instrumental characterization. **Wangxiang Li:** Instrumental characterization. **Elena B. Haddon:** Instrumental characterization. **Boniface P.T. Fokwa:** Software, data curation, draft revision and editing. **Justin Nenwa:** Conceptualization, methodology, supervision, validation, reviewing and editing.

#### Appendix A. Supplementary data

CCDC 2108938 and 2108940 contain supplementary crystallographic data for **1** and **2**. These data can be obtained free of charge from the Cambridge Crystallographic Data Centre via http://www.ccdc.cam.ac.uk/data\_request/cif., or from the Cambridge Crystallographic Data Centre, 12 Union Road, Cambridge CB2 1EZ, UK; fax: (+44) 1223 336 033; or e-mail: deposit@ccdc.cam.ac.uk. mmc1.pdf mmc2.pdf mmc3.cif mmc4.cif mmc5.docx

#### **Declaration of competing interest**

The authors declare that they have no known competing financial interests or personal relationships that could have appeared to influence the work reported in this paper.

#### Acknowledgements

Prof. Boniface P.T. Fokwa gratefully acknowledges financial support by the National Science Foundation Career award no. DMR-1654780. The authors also acknowledge the financial support through Researchers Supporting Project number (RSP-2021/147), King Saud University, Riyadh, Saudi Arabia.

#### Supplementary materials

Supplementary material associated with this article can be found, in the online version, at doi:10.1016/j.molstruc.2022.133528.

#### References

- [1] J.M. Lehn, Angew. Chem. Int. Ed. 29 (1990) 1304.
- [2] I.H. van Esch, Nature 466 (2010) 193.
- [3] F.R. Gamble, F.J. DiSalvo, R.A. Klemm, T.H. Geballe, Science 168 (1970) 568.
- [4] T.M. Reineke, M. Eddaoudi, D. Moler, M. O'Keeffe, O.M. Yaghi, J. Am. Chem. Soc. 122 (2000) 4843.
- [5] L.S. Sapochak, F.E. Benincasa, R.S. Schofield, J.L. Baker, K.K.C. Riccio, D. Fogarty, H. Kohlmann, K.F. Ferris, P.E. Burrows, J. Am. Chem. Soc. 124 (2002) 6119.
- [6] R. Pohl, P.A. Jr, Org. Lett. 5 (2003) 2769.
- [7] X.H. Zhu, J. Peng, Y. Cao, J. Roncali, Chem. Soc. Rev. 40 (2011) 3509.
- [8] B. Zhang, Y. Zhang, Z. Wang, S. Gao, Y. Guo, F. Liu, D. Zhu, CrystEngComm 15 (2013) 3529.
- [9] I. Matulková, J. Cihelka, K. Fejfarová, M. Dušek, M. Pojarová, P. Vanek, J. Kroupa, M. Šála, R. Krupková, I. Nemec, CrystEngComm 13 (2011) 4131.
- [10] M. Clemente-Leon, E. Coronado, J.R. Galan-Mascaros, E. Canadell, Inorg. Chem. 39 (2000) 5394
- [11] E. Coronado, J. Galan-Mascaros, C.J. Gomez-Garcia, V. Laukhin, Nature 408 (2000) 447.
- [12] D.B. Mitzi, S. Wang, C.A. Feild, C.A. Chess, A.M. Guloy, Science 267 (1995) 1473.
- [13] 13 A. Zare, F. Monfared, S.S. Sajadikhah, Appl. Organomet. Chem. (2021) e6046.
- [14] P.G. Lacroix, I. Malfant, S. Bénard, P. Yu, E. Rivière, K. Nakatani, Chem. Mater. 13 (2001) 441.
- [15] M. Clemente-Leon, E. Coronado, C. Marti-Gastaldo, F.M. Romero, Chem. Soc. Rev. 40 (2011) 473.
- [16] B. Zang, Y. Zhang, D. Zhu, Dalton Trans. 41 (2012) 8509.

- [17 D. Gatteschi, R. Sessoli, Angew. Chem. Int. Ed. 42 (2003) 268.
- [18] R. Sessoli, D. Gatteschi, A. Caneschi, M. Novak, Nature 365 (1993) 149.
- [19] Y. Yamamoto, E. Toyota, Bull. Chem. Soc. Jpn 59 (1986) 617.
- [20] W. Kläui, W. Eberspach, P. Gütlich, Inorg. Chem. 26 (1987) 3977.
- [21] S. Nandi, K. Das, A. Datta, S. Roy, E. Garribba, T. Akitsu, C. Sinha, Inorg. Chim. Acta 462 (2017) 75.
- [22] K. Das, A. Datta, A. Pevec, S.B. Mane, M. Rameez, E. Garribba, T. Akitsu, S. Tanka, J. Mol. Struct. 1151 (2018) 198.
- [23] H.B. Lee, N. Ciolkowski, C. Winslow, J. Rittle, Inorg. Chem. 60 (2021) 11830.
- [24] N.M. Ma Houga, F. Capet, J. Nenwa, G. Bebga, M. Foulon, Acta Crystallogr E71 (2015) 1408.
- [25] C.M.N. Choubeu, B.N. Ndosiri, H. Vezin, C. Minaud, J.B. Orton, S.J. Coles, J. Nenwa, J. Coord. Chem. 74 (2021) 1209.
- [26] C.F.N. Nguemdzi, F. Capet, J. Ngoune, G. Bebga, M. Foulon, J. Nenwa, J. Coord. Chem 71 (2018) 1484
- [27] A. Akutsu-Sato, H. Akutsu, S.S. Turner, P. Day, Angew. Chem. Int. Ed. 44 (2005)
- [28] M.M. Bélombé, J. Nenwa, Y.A. Mbiangué, G. Bebga, F. Majoumo-Mbé, E. Hey-Hawkins, P. Lönnecke, Inorg. Chim. Acta 362 (2009) 1.
  [29] C.T. Eboga, G. Bebga, Y.A. Mbiangué, E.N. Nfor, P.L. Djonwouo, M.M. Bélombé, J.
- Nenwa, Open J. Inorg. Chem. 7 (2017) 75
- [30] A.N. Nana, D. Haynes, H. Vezin, C. Minaud, P. Shankhari, B.P.T. Fokwa, J. Nenwa, J. Mol. Struct. 1220 (2020) 128642.
- [31 J.C. Bailar, E.M. Jones, Inorg. Synth. 1 (1939) 35.
- [32] A. Earnshaw, Introduction to Magnetochemistry, Academic Press, London, 1968.
- [33] G.M. Sheldrick, SADABS, University of Göttingen, Göttingen, Germany, 2010.
- [34] G.M. Sheldrick, Acta Crystallogr C71 (2015) 3
- [35] K. Brandenburg, Diamond, Crystal Impact, GbR, Bonn, Germany, 1999.
- [36] S.P. Westrip, J. Appl. Crystallogr. 43 (2010) 920.
- [37] Y. Sun, Y. Zong, H. Ma, A. Zhang, K. Liu, D. Wang, W. Wang, L. Wang, J. Solid State Chem. 237 (2016) 225.
- [38] L. Wang, W. Wang, D. Guo, A. Zhang, Y. Song, Y. Zhang, K. Huang, CrystEng-Comm 16 (2014) 5437.
- [39] J. Nenwa, G. Bebga, P.L. Djonwouo, B.P.T. Fokwa, Res. J. Chem. Environ. 16 (2012) 111.
- [40] M.M. Bélombé, J. Nenwa, O.T. Tene, B.P.T. Fokwa, Glob. J. Inorg. Chem. 1 (2010)
- [41] J. Nenwa, M.M. Bélombé, J. Ngoune, B.P.T. Fokwa, Acta Crystallogr E66 (2010) m1410.
- [42] A. Ghouili, N. Chaari, F. Zouari, X-ray Struct, Anal 26 (2010) x21.
- M. Benslimane, H. Merazig, J.C. Daran, O. Zeghouan, Acta Crystallogr. E68 (2012) m1321.
- [44 M.B. Ben Nasr, F. Lefebvre, C.B. Ben Nasr, Am. J. Anal. Chem. 6 (2015) 446.
- [45 E.D. Djomo, F. Capet, J. Nenwa, M.M. Bélombé, M. Foulon, Acta Crystallogr E71 (2015) 934.
- [46] I.N. Kamga, B.N. Ndosiri, A.N. Nana, T. Roman, L.S. Pouamo, J. Nenwa, Polyhedron 205 (2021) 115291.
- [47] W.W. Wendlandt, E.L. Simmons, J. Inorg. Nucl. Chem. 27 (1965) 2317.
- [48] T.M. Muziol, G. Wrzeezcz, L. Chrzaszcz, Polyhedron 30 (2011) 169.
- A.A. Zolotukhin, A.A. Korshunova, M.P. Bubnov, A.S. Bogomyakov, E.V. Baranov, V.K. Cherkasov, Inorg. Chim. Acta 512 (2020) 119869.